

# EFFECT OF HEATING RATE ON RECRYSTALLIZATION IN ROLLED MULTICRYSTALS OF PURE NIOBIUM\*

T. R. Bieler<sup>†</sup>, N. G. Fleming, D. Kang, C. McKinney, Z. L. Thune, K. Zheng  
Michigan State University, East Lansing, MI, USA

R. Rodríguez-Desconocido, M. Terol-Sánchez, Universidad Polytechnica Madrid, Madrid, Spain  
A. Kolka, Niowave Inc., Lansing, MI, USA

## Abstract

The performance of niobium cavities in superconducting radio frequency particle accelerators requires nearly defect free inner surfaces. While methods to obtain smooth inner surfaces are in place, the role of metallurgical defects on superconducting performance is less known, as defects such as grain boundaries and dislocations can trap flux that dissipates energy and reduces efficiency. Variable microstructure and texture gradients may account for the observed variability in cavity performance, so it is hypothesized that the texture and microstructure gradients originate from the large grain size of ingots, whose influence is not completely erased in the process of making sheet metal. To examine the evolution of microstructure and texture gradients, the crystal orientations present in a cylindrical cap rolled to ~90% reduction were heat treated. Initial crystal orientations were measured before rolling, and before and after slow and rapid heating rate vacuum heat treatments.

## INTRODUCTION

In the past decade, high  $Q$  values have been achieved in high purity Niobium SRF cavities. Trapped flux is a significant factor that degrades  $Q$ , which is associated with defects such as impurities, dislocations, and grain boundaries [1–7]. With a better understanding of the effects of dislocation substructure evolution and recrystallization on electron and phonon transport, as well as the subsurface and surface states, it will be possible to design optimal processing paths for cost effective and high-performance accelerator cavities [8]. Recent experience with cavity production for the LCLS-II has shown that heat treatments at higher temperatures than 800°C are sometimes required to achieve acceptable cavity performance [9]. The higher heat treatment temperatures enhance flux expulsion during the transition to the superconducting state, so that less trapped flux leads to higher  $Q$ , and lower cryogenic costs.

As higher heat treatment temperatures lead to more recrystallization and/or grain growth, and as grain boundary motion leaves a less defective crystal structure in its wake, the ability to achieve microstructures with fewer defects leads to better performance. More importantly, the ability to obtain microstructures that consistently result in sufficient recrystallization and/or grain growth during the final heat

treatment of cavities is important, so that the variability in cavity performance can be reduced. It is well known that the microstructure and properties of the same sheet metal product from the same supplier can vary significantly [8]. To this end, it is important to examine how the path from ingot to sheet metal leads to the variable microstructures and properties that affect cavity forming and subsequent changes during heat treatment.

Prior examination of the deformation characteristics of pure niobium single and multicrystals shows that some crystal orientations result in uniform deformation at the microscale while others lead to very heterogeneous deformation [10–14]. In these investigations, the recrystallization was very sensitive to the both the crystal orientation and the heat treatment temperature. An important factor to consider is that recovery (reduction of dislocation density and formation of stable low-angle grain boundaries) takes place both during plastic deformation and during heat treatment [4–6]. If too much recovery takes place, the driving force for recrystallization is reduced, i.e. if high-angle grain boundaries do not move, the stable low angle boundaries are retained. As both low angle and high angle boundaries can trap flux [3–7], it is strategic to minimize both without compromising the strength required to maintain the cavity shape.

This paper focuses on the relationship between the amount of rolling reduction, crystal orientation and heat treatment parameters and their effect on recrystallization in order to improve our general understanding of why microstructures are so variable in rolled sheet metal. With improved understanding, it may be possible to identify better processing paths that will lead to more meaningful acceptance criteria for sheet metal that will lead to consistent recrystallization during heat treatments such that cavity performance will be more consistent.

## EXPERIMENTAL PROCEDURES

A cylindrical cap in Fig. 1 of high RRR niobium was obtained from an ingot (Niowave Inc., Lansing MI). Prior to rolling, two slices were cut off the edges to measure the orientation of grains on each side of the sample using Laue X-ray diffraction (Fig. 2), indicating that the grain orientations on both sides were different. About 25 passes were used with 10% reduction of the current thickness per pass, resulting in about 90% reduction. The orientations near the surface experience a greater amount of shear than the interior, as indicated by the sketch on the left side of Fig. 1. The rolling process led to one side of the strip being more reduced than the other, causing a curve in the rolled strip, such that it had

\* This work is supported by US Dept. of Energy award DE-SC0009960. Some of this work was conducted during a sabbatical leave of TRB that was supported by the Talent Attraction program of the Comunidad de Madrid (reference 2016-T3/IND-1600).

<sup>†</sup> [tbler@egr.msu.edu](mailto:tbler@egr.msu.edu)

to be cut in half part way through the rolling process in order to continue to reduce it (Fig. 1). Assuming uniform reduction (which was clearly not the case), the approximate positions of the different grains were identified in the % reduction vs. position plot in Fig. 2 (note that the % reduction varies along the position due to the initial geometry). Based upon this estimate, pieces of the rolled sheet were removed at locations that included a grain boundary, which was sometimes visible on the surface of the sheet after it was etched. At each location, five 1 mm thick x 3 mm wide x 25 mm long samples were cut out using EDM to obtain pieces with nominally similar microstructures that could be heat treated in different ways.

The small samples were immersed in a buffered chemical polish to remove 5-10 μm of the EDM recast surface. The surface finish was smooth enough to obtain EBSD maps without any other surface preparation for most of the regions in the samples, but some regions such as the middle of A6 with >90% reduction revealed only about half of the orientations, as shown in Fig. 3.

Selected samples were given a vacuum heat treatment with a 3 hr ramp to 1000°C with a 3 hr hold at Jefferson National Accelerator Facility. Other samples were encapsulated in fused silica tubes with a rough vacuum and heat treated in a box furnace using a 3 hour ramp to 900°C with a 3 hour hold. Some samples were given a much faster heating rate by placing the encapsulated samples into the furnace shortly before the ramp reached the target temperature.

## RESULTS AND DISCUSSION

Figure 3 shows the grain reference orientation deviation (GROD) map for the heat-treated A6 sample, which is based upon the minimum kernel average misorientation in each grain, using a color scale that represents up to 60° misorientation within a given grain. The upper part is recrystallized, with each grain surrounded by black high-angle (>15°) boundaries in both the IPF map and the GROD map (recrystallized grains have a uniform blue color implying no orientation gradients in the grain). The lower quarter

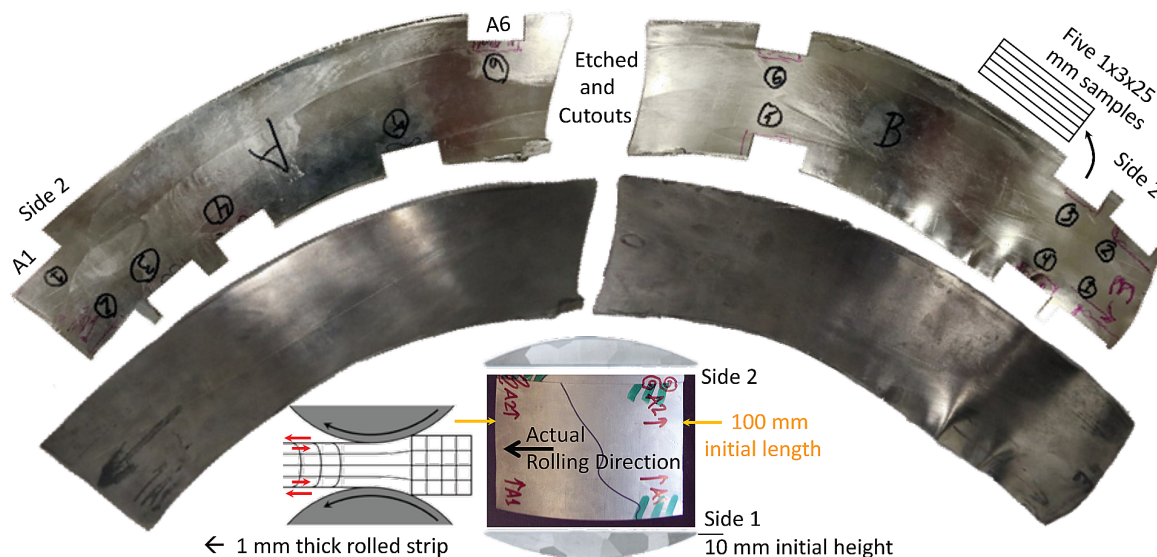


Figure 1: A cylindrical cap from an ingot that was rolled and slices of the edges that reveal the grain structure – it curved due to different resistance to deformation on the two sides of the piece. Cutouts were made near the original grain boundaries to provide multiple 1 x 3 x 25 mm samples for different heat treatments.

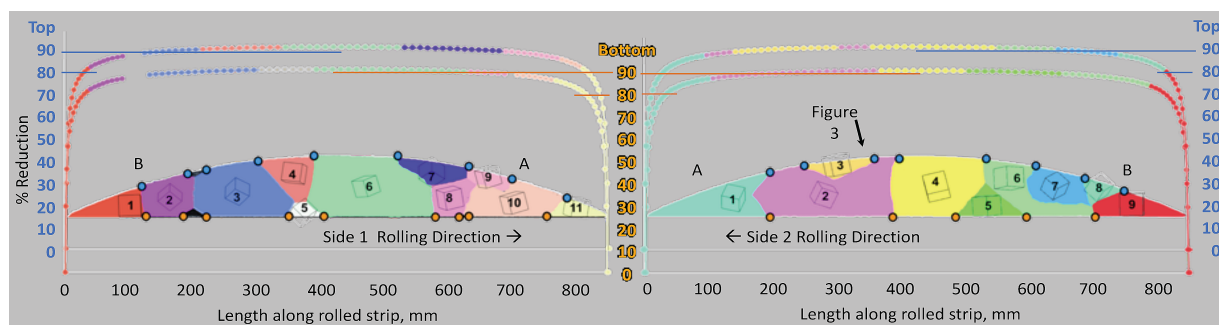


Figure 2: Orientations of crystals within the cylindrical cap on side 1 and 2 from the perspective of looking outward from the centerline of the strip, and the approximate locations of prior grain boundaries on the top and bottom of the reduced thickness of the rolled cylindrical cap. The curve for the top (blue scale) is displaced above the curve for the bottom to avoid overlap.



Content from this work may be used under the terms of the CC BY 4.0 licence (© 2022). Any distribution of this work must maintain attribution to the author(s), title of the work, publisher, and DOI

recovered rather than recrystallized, as indicated by color gradients and lack of black boundaries [15].

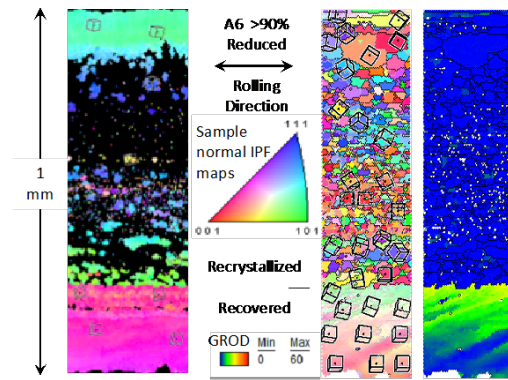


Figure 3: As-rolled sample A6 shows partial EBSD measurement due to surface roughness resulting from removing  $\sim 5\text{-}10\ \mu\text{m}$  using BCP. After  $1000^\circ\text{C}$  recrystallization, the sample was polished, revealing a mostly recrystallized microstructure, but the lower magenta grain showed only recovery. Dark blue on the GROD map represents the orientation within each grain with the least lattice curvature. The color scales and dimensions noted here apply to subsequent figures.

Figure 4 illustrates the microstructure of sample A1 at about 20%, 70% and 80% reduction. Orientation (color) gradients developed with  $\sim 20\%$  reduction, and new orientations developed by rotation of regions away from the majority aqua colored orientation that maintained nearly the same orientation with increasing strain up to  $\sim 80\%$  reduction. Within the aqua region, a gold rotation band (also evident on the bottom of the  $\sim 20\%$  reduction area) rotated counter-clockwise as sketched in the GROD map and also rotated about an  $\langle 001 \rangle$  axis that is parallel to the surface. The magnitude of orientation gradients is more clearly revealed in the GROD

maps. In the 80% reduced region, there is an oscillating orientation gradient near the top and bottom, which leads to a cumulative gradient of  $60^\circ$  from the lower (dark blue) region to the red region at the top. While there are many low-angle grain boundaries in the IPF maps (gray lines), there is no black high-angle grain boundary, so the entire volume is still considered a single grain with a long-range gradient.

Following the  $1000^\circ\text{C}$  heat treatment, the micro structure of the same grain (on a different nearby sample) shows little change from the as-rolled microstructure. This implies that recovery rather than recrystallization occurred, as no mobile high angle boundaries swept away the GND content. Only in the 80% reduced material was there enough stored energy to enable high angle boundaries to migrate and cause recrystallization near the upper surface where there are several uniformly dark blue grains on the GROD map. These grains have different orientations (colors on the IPF map). Also, the gold rotation band recrystallized into orientations similar to the original rotation band, with wavy boundaries indicative of strain induced grain boundary migration, where dislocation content in the aqua grain attracted migration of the gold grain boundary into the aqua grain until there was not enough dislocation content to attract it deeper into the aqua grain. The large red region is misoriented about  $60^\circ$  from the dark blue orientation in the lower left corner, which did not recrystallize, but only recovered, as there are smooth color gradients that can be followed continuously from this corner. In the lower right near the IPF yellow region, there is a small dark blue grain which is probably not recrystallized, as it is not surrounded by a black line in the IPF map.

The  $1000^\circ\text{C}$  heat treatment in A6 caused recrystallization in the top and center region (Fig. 3, and see the arrow pointing to this location in Fig. 2). The green orientation at the top of the undeformed region is similar to the yellow-orange

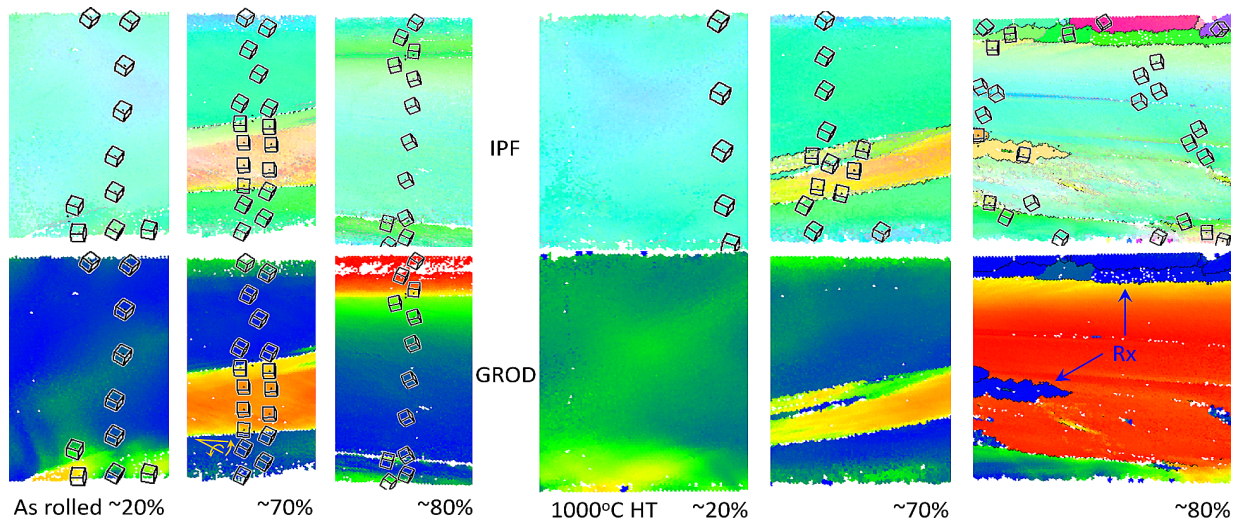


Figure 4: As-rolled sample A1 with increasing reduction shows heterogeneous rotations that develop a  $30\text{-}35^\circ$  gold misorientation band within a stable aqua orientation. After heat treatment at  $1000^\circ\text{C}$ , recrystallization only occurred in some locations in the  $\sim 80\%$  reduced orientation along the top and within the gold misorientation band. Maps have the same color scales as in Fig. 3.

orientation initially present on the top. The magenta and aqua colors on the top and bottom both have a near-[001] direction perpendicular to the sheet surface, indicating that such orientations are stable under conditions of shear. Apparently, the rotated cube orientation on the top was in a better condition to recrystallize, while the magenta orientation on the bottom that is closer to a cube orientation was resistant to recrystallization, so it recovered, as indicated by orientation gradients in the lower part. In the deformed state, only the lower part of the grain has an orientation close to the initial magenta orientation, and the inner part of the grain has many other orientations that may have formed similarly to the gold rotation band. There is a distinct boundary between the magenta grain and mostly green and blue orientations in the poorly measured area. This boundary is also bulged, indicating that the recrystallized grains were growing into the magenta grain, but did not progress due to a lack of sufficient defect content in the magenta grain.

Two additional samples annealed at 900°C from A1 are shown in Fig. 5, but they had different heating rates and prior history. The same features are present as in Fig. 4 in most of the maps, and the main difference between them is that no recrystallization was observed with the fast heating rate, but this sample had been previously heat treated with a slow heating rate to 800°C for 3 hrs. The slow heating rate showed a little bit of recrystallization (dark blue elongated grains in the GROD map in the 80% reduced maps). As in the 1000°C heat treatment, recrystallization nucleated in the yellow bands, but was not able to grow into the aqua orientation effectively. This provides evidence that the yellow band probably had a higher dislocation density, that enabled nucleation of grains that grew along the yellow band, but due to a lower dislocation density in the aqua region, they were confined to the yellow band. The yellow bands in the IPF maps have black boundaries, indicating that the interface

is sharp rather than diffuse. There is also a black boundary separating the yellow and green (not aqua) orientation. The boundary in a similar position in the fast heating sample had not quite formed a continuous high angle boundary, perhaps because the recovered microstructure was stabilized by the prior 800°C heat treatment.

The yellow rotation band recrystallized preferentially due to a higher density of dislocations, indicating that formation of this band represents a plastic instability. A generalized Schmid factor analysis based upon “plane strain compression” of the aqua, yellow and green orientations in Fig. 6 shows the four most favored slip systems. The yellow and green orientations have slip systems with higher Schmid factors (more easily activated) than the aqua orientations, so when the aqua orientation rotated toward these orientations, they became easier to deform and generated more dislocations. These illustrate how banded heterogeneous microstructures develop while in making sheet metal from large grains. This heterogeneous strain leads to gradients in crystal orientations, grain size, and amount of retained non-recrystallized (recovered) grains. In the 80% strained A1 samples, relatively sharp orientation gradients develop about a third of the way from the surface to the center, which may be where a transition in stress state takes place between predominantly shear deformation near the surface and the ‘plane strain compression’ that is associated with rolling.

Interestingly, very little recrystallization can take place in large grain material, in contrast to a companion paper where a 30% reduction of an annealed piece of polycrystalline sheet can recrystallize to a much greater degree at 900 or 1000° [16]. In another related study comparing the ‘damage layer that develops due to friction from the die when forming SRF cavities, much larger orientation gradients develop in a polycrystal than in a large grain material [17, 18]. Grain boundaries are clearly helpful for obtaining conditions for

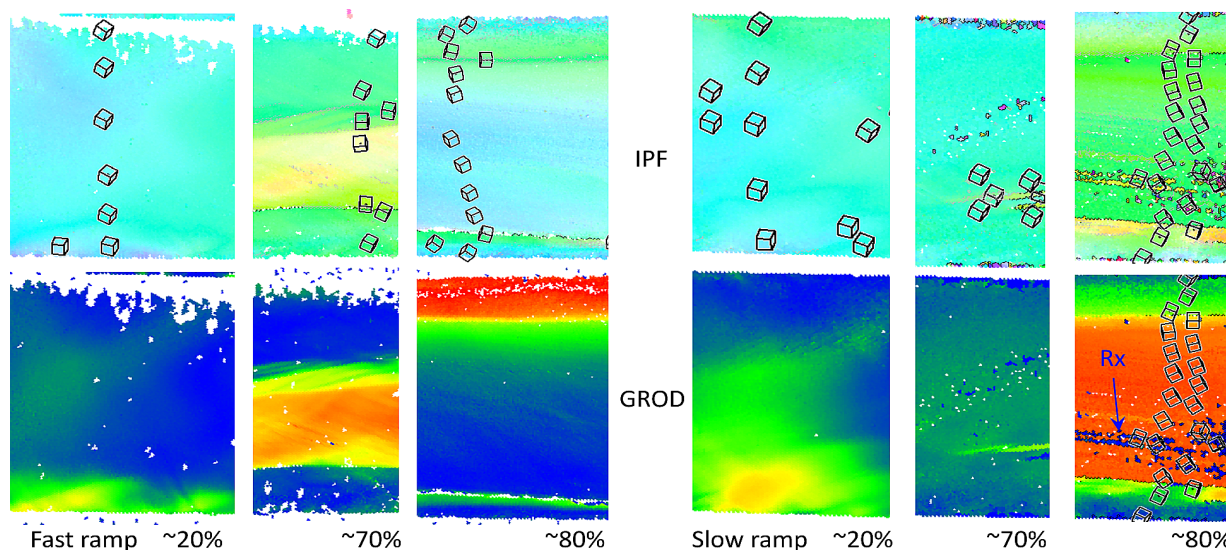


Figure 5: Two different but neighboring samples from A1 similar to Fig. 4 were heated to 900°C at a fast ramp rate and a slow ramp rate. The fast heating rate sample had a prior heat treatment at 800°C, and no recrystallization occurred. The slow ramp sample recrystallized only along yellow deformation/rotation bands in the ~80% region.



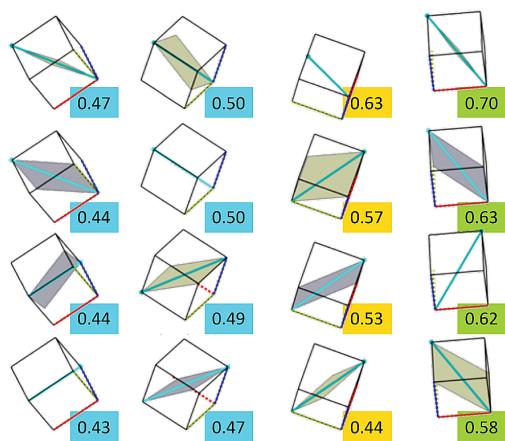


Figure 6: : The generalized Schmid factors (higher values imply easier deformation) for plane strain compression of the four most favored slip systems (turquoise slip vector on shaded plane) for exemplary orientations in A1 are illustrated; the aqua orientations are harder, such that rotations toward the yellow or green orientations lead to a plastic instability that reduces the local stress needed to deform the material.

recrystallization, as high angle boundaries are plentiful, but they are not plentiful in large grain material. Thus, heat treatments of deformed large grain material are much more likely to recover than recrystallize.

## CONCLUSIONS

Development of orientation gradients during rolling of large grain material leads to orientation banding that leads to softer orientations, plastic instabilities and heterogeneous deformation. Subsequent heat treatments cause heterogeneous microstructures and property variability. Recrystallization is very sensitive to strain and crystal orientation. For the samples examined here, a rapid heating rate did not enhance recrystallization as it did in a polycrystal [16]. Similar experiments on the other samples are under way.

## REFERENCES

- [1] G. Ciovati and A. Gurevich, "Evidence of high-field radio-frequency hot spots due to trapped vortices in niobium cavities," *Phys. Rev. Accel. Beams*, vol. 11, p. 122001, 2008. doi:10.1103/PhysRevSTAB.11.122001
- [2] S. Posen *et al.*, "The Effect of Mechanical Cold Work on the Magnetic Flux Expulsion of Niobium", 2019. arXiv:1804.07207
- [3] A. A. Polyanskii *et al.*, "Magneto-Optical Study High-Purity Niobium for Superconducting RF Application", in *AIP Conf. Proc.*, vol. 1352, pp. 186–202, 2011. doi:10.1063/1.3579237
- [4] M. Wang *et al.*, "Investigation of the Effect of Strategically Selected Grain Boundaries on Superconducting Properties of High Purity Niobium", in *Proc. 18th Int. Conf. RF Superconductivity (SRF'17)*, Lanzhou, China, pp. 787–791, Jul. 2017. doi:10.18429/JACoW-SRF2017-THPB026
- [5] Z. H. Sung *et al.*, "Development of low angle grain boundaries in lightly deformed superconducting niobium and their influ-

- ence on hydride distribution and flux perturbation", *J. App. Phys.*, vol. 121, p. 193903, 2017. doi:10.1063/1.4983512
- [6] M. Wang, D. Kang, and T. R. Bieler, "Direct observation of dislocation structure evolution in SRF cavity niobium using electron channeling contrast imaging", *J. App. Phys.*, vol. 124, p. 155105, 2018. doi:10.1063/1.5050032
- [7] M. Wang *et al.*, "Study of Dislocation Content Near Grain Boundaries Using Electron Channeling Contrast Imaging and its Effect on the Superconducting Properties of Niobium", in *Proc. 19th Int. Conf. RF Superconductivity (SRF'19)*, Dresden, Germany, pp. 876–880, 2019. doi:10.18429/JACoW-SRF2019-THP020
- [8] T.R. Bieler *et al.*, "Physical and mechanical metallurgy of high purity Nb for accelerator cavities," *Phys. Rev. Accel. Beams*, vol. 13, p. 31002, 2010. doi:10.1103/PhysRevSTAB.13.031002
- [9] S. Posen *et al.*, "Role of magnetic flux expulsion to reach  $Q_0 > 3 \times 10^{10}$  in superconducting rf cryomodules", *Phys. Rev. Accel. Beams*, vol. 22, p. 032001, 2019. doi:10.1103/PhysRevAccelBeams.22.032001
- [10] H. R. Z. Sandim, J. F. C. Lins, A. L. Pinto, and A. F. Padilha, "Recrystallization behavior of a cold-rolled niobium bicrystal", *Mater. Sci. Eng. A*, vol. 354, pp. 217–228, 2003. doi:10.1016/S0921-5093(03)00011-X
- [11] H. R. Z. Sandim and D. Raabe, "An EBSD Study on Orientation Effects During Recrystallization of Coarse-Grained Niobium", *Mater. Sci. Forum*, vol. 467–470, pp. 519–524, 2004. doi:10.4028/www.scientific.net/MSF.467-470.519
- [12] H. R. Z. Sandim, and D. Raabe, "EBSD study of grain subdivision of a Goss grain in coarse-grained cold-rolled niobium", *Scripta Mater*, vol. 53 pp. 207–212, 2005. doi:10.1016/j.scriptamat.2005.03.045
- [13] H. R. Z. Sandim, H. H. Bernardi, B. Verlinden, and D. Raabe, "Equal channel angular extrusion of niobium single crystals", *Mater. Sci. Eng. A*, vol. 467 pp. 44–52, 2007. doi:10.1016/j.msea.2007.02.086
- [14] L. Zhu, H. R. Z. Sandim, M. Seefeldt, B. Verlinden, "Grain Subdivision of a Nb Polycrystal Deformed by Successive Compression Tests", *Mater. Sci. Forum*, vol. 667–669, pp. 373–378, 2011. doi:10.4028/www.scientific.net/MSF.667-669.373
- [15] R. D. Doherty *et al.*, "Current issues in recrystallization: A review", *Mater. Sci. Eng. A*, vol. 238, pp. 219–274, 1997. doi:10.1016/S0921-5093(97)00424-3
- [16] Z. L. Thune, N. G. Fleming, C. McKinney, E. M. Nicometo, S. Balachandran, and T. R. Bieler, "Ex-Situ Investigation of the Effects of Heating Rate on the Recrystallization in Rolled Polycrystals of High-Purity Niobium", presented at the 20th International Conference on RF Superconductivity (SRF21), June 2021, paper SUPCAV002, this conference.
- [17] E. M. Nicometo, Z. L. Thune, I. Jarvis, G. Ereemeev, and T. R. Bieler, "The Influence of Local Deformation from Forming on Recovery and Recrystallization in Deformed Polycrystal Niobium SRF Cavities", presented at the 20th International Conference on RF Superconductivity (SRF21), June 2021, paper SUPCAV012, this conference.
- [18] D. Kang, T. R. Bieler, and C. Compton, "Effects of processing history on the evolution of surface damage layer and dislocation substructure in large grain niobium cavities," *Phys. Rev. Accel. Beams*, vol. 18, p. 123501, Dec. 2015. doi:10.1103/PhysRevSTAB.18.123501.